

Search for Top Quark FCNC Couplings in Z' Models at the LHC and CLIC

O. Çakır*

*Ankara University, Faculty of Sciences,
Department of Physics, 06100, Tandogan, Ankara, Turkey*

I.T. Çakır†

Physics Department, CERN, 1211, Geneva 23, Switzerland

A. Senol‡ and A.T. Tasci§

*Kastamonu University, Faculty of Arts and Sciences,
Department of Physics, 37100, Kuzeykent, Kastamonu, Turkey*

Abstract

The top quark is the heaviest particle to date discovered, with a mass close to the electroweak symmetry breaking scale. It is expected that the top quark would be sensitive to the new physics at the TeV scale. One of the most important aspects of the top quark physics can be the investigation of the possible anomalous couplings. Here, we study the top quark flavor changing neutral current (FCNC) couplings via the extra gauge boson Z' at the Large Hadron Collider (LHC) and the Compact Linear Collider (CLIC) energies. We calculate the total cross sections for the signal and the corresponding Standard Model (SM) background processes. For an FCNC mixing parameter $x = 0.2$ and the sequential Z' mass of 1 TeV, we find the single top quark FCNC production cross sections 0.38(1.76) fb at the LHC with $\sqrt{s_{pp}} = 7(14)$ TeV, respectively. For the resonance production of sequential Z' boson and decays to single top quark at the Compact Linear Collider (CLIC) energies, including the initial state radiation and beamstrahlung effects, we find the cross section 27.96(0.91) fb at $\sqrt{s_{e^+e^-}} = 1(3)$ TeV, respectively. We make the analysis to investigate the parameter space (mixing-mass) through various Z' models. It is shown that the results benefit from the flavor tagging.

PACS numbers: 12.60.Cn, 14.70.Pw, 14.65.Ha

*Electronic address: ocakir@science.ankara.edu.tr

†Electronic address: tcakir@mail.cern.ch

‡Electronic address: asenol@kastamonu.edu.tr

§Electronic address: atasci@kastamonu.edu.tr

I. INTRODUCTION

The top quark is a wonderful probe for the new physics beyond the Standard Model (SM) via its decays and productions at high energy colliders. At the Large Hadron Collider (LHC) the top quark events will be produced copiously. We may anticipate the discovery of new physics by observing the anomalous couplings in the top quark sector. The flavour changing neutral currents (FCNC) couplings of the top quark can also be enhanced to observable levels in some new physics models. Many extensions of the SM predict the extra gauge bosons, especially the Z' -boson has been the object of extensive phenomenological studies ([1] and references therein). An extra $U(1)$ gauge boson Z' can induce flavor changing neutral currents. In the models with an extra $U(1)$ group the Z' boson can have tree-level or an effective $Z' - q - q'$ couplings, where q and q' are both the up-type quarks or down-type quarks. The LHC can probe some parameter space of the Z' models provided necessary luminosity. If a Z' boson is found at the LHC, the underlying model could be best identified at the linear colliders through the polarization observables.

The current experimental searches of the Z' boson from Drell-Yan cross sections at Tevatron have put lower limits on the mass range $0.6 - 1.0$ TeV at 95% C.L. depending on the specific Z' models [2]. From the electroweak precision data analysis, the improved lower limits on the Z' mass are given in the range $1.1 - 1.4$ TeV at 95% C.L. [3]. These limits on the Z' boson mass favors higher energy (≥ 1 TeV) collisions for direct observation of the signal. It is also possible that the Z' bosons can be much heavy or weak enough to escape beyond the discovery reach expected at the LHC. In this case, only the indirect signatures of Z' exchanges may occur at the high energy colliders.

The Z' models have some special names [2]: sequential Z'_S model has the same couplings to the fermions as that of the Z boson of the SM, left-right symmetric Z'_{LR} model has the couplings a combination of right-handed and $B - L$ neutral currents, the Z'_ψ , Z'_χ and Z'_η models corresponding to the specific values of the mixing angle in the E_6 model have different couplings to the fermions.

A work which addresses the effects of tree-level FCNC interactions induced by an additional Z' boson on the single top quark production at the LHC ($\sqrt{s} = 14$ TeV) and International Linear Collider (ILC) ($\sqrt{s} = 1$ TeV) has been performed in Ref. [4]. In the paper, the relevant signal cross sections have been calculated and especially the charm tagging

to identify the signal has been discussed. Even though it shows the potential of the LHC and ILC for a certain parameter set in the single top FCNC production, it is free of a detailed analysis for the background, including Monte Carlo (MC) simulation and observability for a full parameter space.

In our work, we investigate both the single and pair production of top quarks via FCNC interactions through Z' boson exchange at the LHC and Compact Linear Collider (CLIC) [5]. The aim of this paper is to complement the previous other works by studying the signal and background in detail in the same MC framework. Therefore, we implement the related interaction vertices into the MC software, and study the FCNC parameters in detail as well as the effects of initial state radiation (ISR) and beamstrahlung (BS) in the e^+e^- collisions. Another feature of our work is that we analyze the signal observability (via contour plots) for the Z' boson and top quark FCNC interactions.

In section II, we calculate the decay widths of Z' boson for the mass range 1000-3000 GeV in the framework of the model which has already been detailed in Ref. [4]. An analysis of the mass and coupling strength parameter space for different Z' models are given for the single and pair production of top quarks at the LHC in section III and at the CLIC in section IV. Taking into account the initial state radiation (ISR) and beamstrahlung (BS) effects in the e^+e^- collisions, we analyzed the signal observability for the Z' boson and top quark FCNC interactions. In order to enrich the signal statistics even at the small couplings we consider both $t\bar{c}$ and $\bar{t}c$ single top productions in the final state. The analysis for the signal significance and conclusion are given in sections V and VI, respectively.

II. MODEL

In the gauge eigenstate basis, following the formalism given in Ref. [4, 6, 7], the additional neutral current Lagrangian associated with the $U(1)'$ gauge symmetry can be written as

$$\mathcal{L}' = -g' \sum_{f,f'} \bar{f} \gamma^\mu \left[\epsilon'_L(ff') P_L + \epsilon'_R(ff') P_R \right] f' Z'_\mu \quad (1)$$

where $\epsilon'_{L,R}(ff')$ are the chiral couplings of Z' boson with fermions f and f' . The g' is the gauge coupling of the $U(1)'$, and $P_{R,L} = (1 \pm \gamma^5)/2$. Here, we assume that there is no mixing between the Z and Z' bosons as favored by the precision data. Flavor changing neutral currents (FCNCs) arise if the chiral couplings are nondiagonal matrices. In case the Z'

couplings are diagonal but nonuniversal, flavor changing couplings are emerged by fermion mixing. In the interaction basis the FCNC for the up-type quarks are given by

$$\mathcal{J}_{FCNC}^{u'} = (\bar{u}, \bar{c}, \bar{t}) \gamma_\mu (\epsilon_L^{u'} P_L + \epsilon_R^{u'} P_R) \begin{pmatrix} u \\ c \\ t \end{pmatrix} \quad (2)$$

where the chiral couplings are given by [4]

$$\epsilon_L^{u'} = C_L^u \begin{pmatrix} 1 & 0 & 0 \\ 0 & 1 & 0 \\ 0 & 0 & x \end{pmatrix} \quad \text{and} \quad \epsilon_R^{u'} = C_R^u \begin{pmatrix} 1 & 0 & 0 \\ 0 & 1 & 0 \\ 0 & 0 & 1 \end{pmatrix}. \quad (3)$$

In general, the effects of these FCNCs may occur both in the up-type sector and down-type sector after diagonalizing their mass matrices. For the right-handed up-sector and down-sector one assumes that the neutral current couplings to Z' are family universal and flavor diagonal in the interaction basis. In this case, unitary rotations ($V_{L,R}^f$) can keep the right handed couplings flavor diagonal, and left handed sector becomes nondiagonal. The chiral couplings of Z' in the fermion mass eigenstate basis are given by

$$B_L^{ff'} \equiv V_L^f \epsilon_L^{f'} (ff') V_L^{f\dagger} \quad \text{and} \quad B_R^{ff'} \equiv V_R^f \epsilon_R^{f'} (ff') V_R^{f\dagger} \quad (4)$$

here the CKM matrix can be written as $V_{CKM} = V_L^u V_L^{d\dagger}$ with the assumption that the down-sector has no mixing. The flavor mixing in the left-handed quark fields is simply related to V_{CKM} , assuming the up sector diagonalization and unitarity of the CKM matrix one can find the couplings [4]

$$B_L^u \equiv V_{CKM}^\dagger \epsilon_L^{u'} V_{CKM} \approx \begin{pmatrix} 1 & (x-1)V_{ub}V_{cb}^* & (x-1)V_{ub}V_{tb}^* \\ (x-1)V_{cb}V_{ub}^* & 1 & (x-1)V_{cb}V_{tb}^* \\ (x-1)V_{tb}V_{ub}^* & (x-1)V_{tb}V_{cb}^* & x \end{pmatrix}. \quad (5)$$

The FCNC effects from the Z' mediation have been studied for the down-type sector and implications in flavor physics [7–17] and up-type sector in top quark production [4, 18–22]. The parameters for different Z' models are given in Table I. In numerical calculations, we take the coupling $g' \simeq 0.65$ for the sequential model and $g' \simeq 0.40$ for other models. In the left-right symmetric model we use $g_L = g_R$, and the chiral couplings $C_L^f = -\sqrt{3/5}(B -$

Table I: The chiral couplings for different Z' models.

	Z'_S	Z'_{LR}	Z'_χ	Z'_ψ	Z'_η
C_L^u	0.3456	-0.08493	$-1/2\sqrt{10}$	$1/\sqrt{24}$	$-1/\sqrt{15}$
C_R^u	-0.1544	0.5038	$1/2\sqrt{10}$	$-1/\sqrt{24}$	$1/\sqrt{15}$
C_L^d	-0.4228	-0.08493	$-1/2\sqrt{10}$	$1/\sqrt{24}$	$-1/\sqrt{15}$
C_R^d	0.0772	-0.6736	$-3/2\sqrt{10}$	$-1/\sqrt{24}$	$-1/2\sqrt{15}$
C_L^e	-0.2684	0.2548	$3/2\sqrt{10}$	$1/\sqrt{24}$	$1/2\sqrt{15}$
C_R^e	0.2316	-0.3339	$1/2\sqrt{10}$	$-1/\sqrt{24}$	$1/\sqrt{15}$
C_L^ν	0.5	0.2548	$3/2\sqrt{10}$	$1/\sqrt{24}$	$1/2\sqrt{15}$

Table II: The Z' boson decay widths (in GeV) for different mass values in the various models with $x = 0.2$ (where the numbers in the paranthesis denotes the values for $x = 1$).

$M_{Z'}(\text{GeV})$	Z'_S	Z'_{LR}	Z'_χ	Z'_ψ	Z'_η
1000	27.36(29.49)	20.08(20.09)	11.39(11.55)	4.90(5.16)	5.73(6.14)
1500	41.13(44.65)	30.30(30.35)	17.11(17.38)	7.39(7.84)	8.65(9.38)
2000	54.87(59.72)	40.49(40.58)	22.83(23.21)	9.87(10.50)	11.57(12.58)
2500	68.62(74.76)	50.66(50.78)	28.54(29.03)	12.35(13.16)	14.47(15.77)
3000	82.35(89.79)	60.82(60.98)	34.26(34.85)	14.82(15.81)	17.38(18.96)

$L)/2\alpha_{LR}$ and $C_R^f = \sqrt{3/5}(\alpha_{LR}I_{3R}^f) + C_L^f$ where the parameter $\alpha_{LR} \simeq 1.52$. Here, the B and L denote the baryon and lepton numbers of the corresponding fermion.

For numerical calculations we have implemented the $Z' - q - q'$ interaction vertices into the CompHEP package [23]. The decay widths of Z' boson for different mass values in the sequential model, LR symmetric model and E_6 -inspired models are given in Table II. For the parameter $x = 1$, both the left-handed and right-handed couplings become universal, and family diagonal. In this case we cannot see the FCNC effects on the decay widths and cross sections. In order to include a little from these effects on the decay width, we take the parameter $x = 0.2$ as shown in Fig. 1. The effect of this FCNC reduces the decay width at most 10% for the sequential model in the relevant mass range. The decay widths are compared with the similar results from Ref. [4] for $x = 0.1$ to prove the implementation.

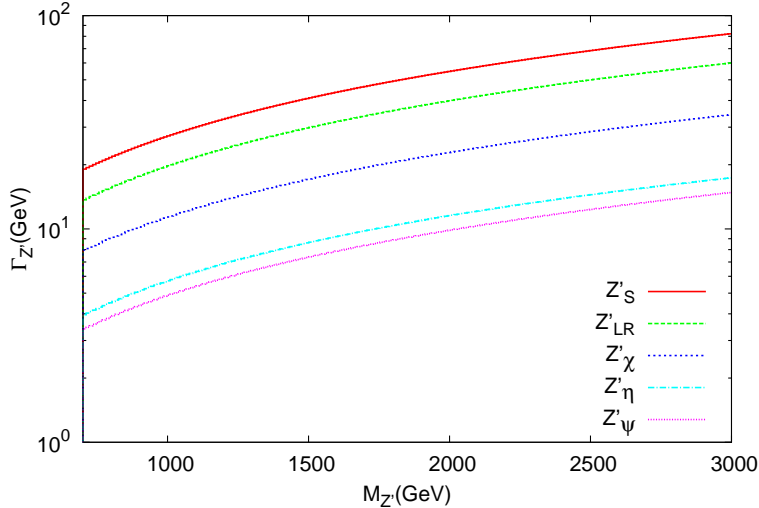


Figure 1: The decay widths of Z' boson depending on its mass for different models with the FCNC parameter $x = 0.2$.

III. PROTON-PROTON COLLISIONS

A. The single top quark production

The cross sections for the process $pp \rightarrow (t\bar{c} + \bar{t}c)X$ depending on the Z' boson mass at the LHC (both for 7 TeV and 14 TeV) are given in Fig. 2 by using parton distribution function library CTEQ6L [24]. Here, the Z' boson contributes through the s - and t -channel diagrams, and the associated production of single top quarks in the final state $t\bar{c}$ well dominates over the tc final state. For this process the cross section at $\sqrt{s} = 14$ TeV is about 3 times larger than the case at $\sqrt{s} = 7$ TeV. Here, we also check our results for $x = 0.1$ which agrees with that of the results of Ref. [4].

The rapidity distribution of the charm quarks (c and \bar{c}) from the signal are shown in Fig. 3 at the collision energy of 14 TeV. We sum up the c and \bar{c} distributions, since there will be no clear difference for them. There is a peak in the c -quark rapidity distribution $\eta^c \simeq 0$ with the tails extending to $|\eta^c| \simeq 2.5$. We may apply a rapidity cut $|\eta^j| < 2.5$ for the signal and background analysis. The rapidity distribution of final state c quarks in the background process $pp \rightarrow (t\bar{c} + \bar{t}c)X$ is shown in Fig. 4.

Fig. 5 shows the p_T distributions of the c -quark in the signal process with $M_{Z'} = 1.5$ TeV for the parameter $x = 0.2$ at the pp center of mass energy of 14 TeV. A high p_T cut

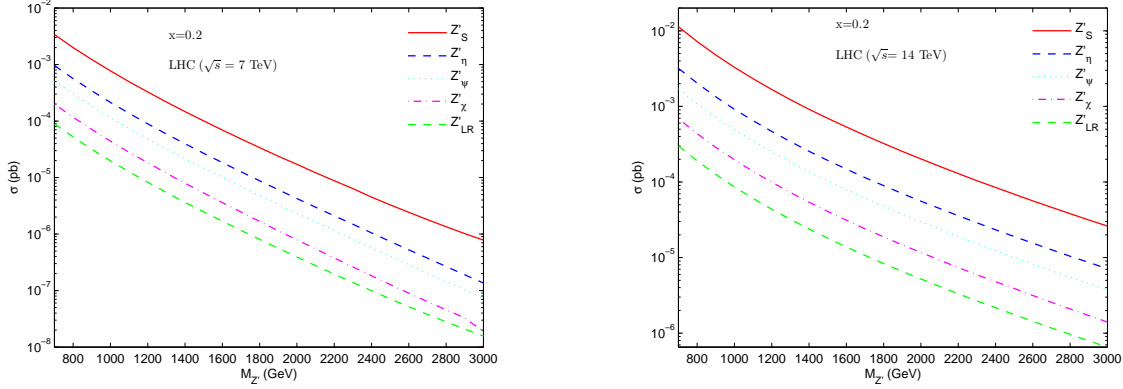


Figure 2: The cross sections for $pp \rightarrow (t\bar{c} + \bar{t}c)X$ versus the Z' boson mass at the LHC ($\sqrt{s} = 7$ TeV left and 14 TeV right). The lines are for the five Z' models explained in the text.

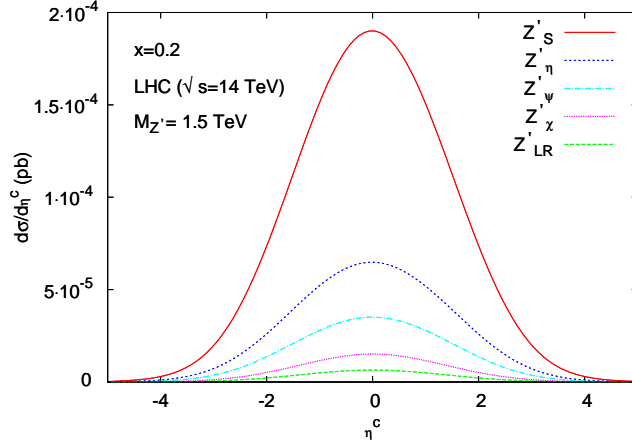


Figure 3: The rapidity distributions of the charm quarks (c and \bar{c}) at the LHC with the center of mass energy of 14 TeV. Here, we take the mass $M_{Z'} = 1.5$ TeV and the FCNC parameter $x = 0.2$.

($p_T > M_{Z'}/2 - 4\Gamma_{Z'}$) reduces the background significantly without affecting much the signal cross section in the interested Z' mass range. The p_T distribution of the c -quark from the background is shown in Fig. 6. We may apply these cuts to make analyses with the signal and background.

We plot the invariant mass distribution of the $W^+b\bar{c}$ system for the signal (sequential model with $x = 0.2$ and $M_{Z'} = 1, 2$ and 3 TeV) and background at the LHC with $\sqrt{s} = 14$ TeV in Fig. 7.

Here, we consider two types of backgrounds for the analysis. The first one has the same final state ($t\bar{c}$ and $\bar{t}c$) as expected for the signal processes and the other one (single top

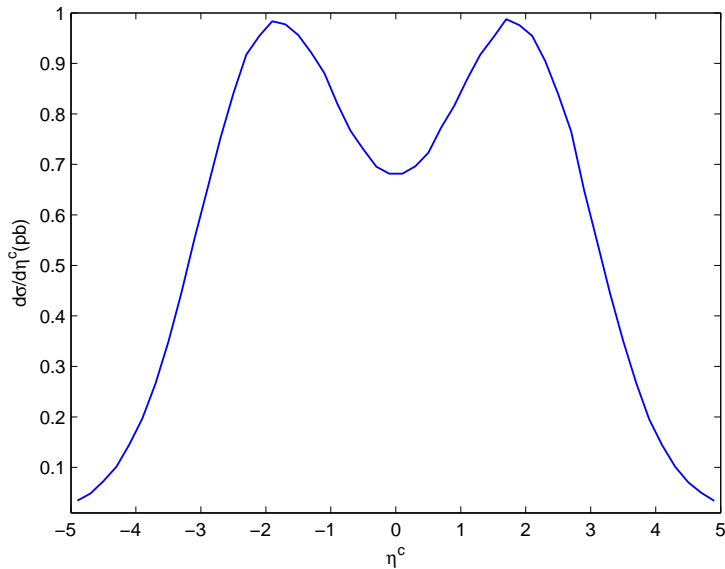


Figure 4: The rapidity distribution of the charm quarks (c and \bar{c}) for the background process ($pp \rightarrow (t\bar{c} + \bar{t}c)X$) at the LHC with $\sqrt{s} = 14$ TeV.

associated with a b -jet) is the irreducible background and contributes to the similar final state, assuming the b -quark which may be misidentified as the charmed jet. One can apply very high transverse momentum (p_T) cut for the b -jets and c -jets. Employing the variable p_T cuts such that $p_T > M_{Z'}/2 - 4\Gamma_{Z'}$ for different Z' mass values and the rapidity cuts $|\eta| < 2.5$ for the central detector coverage, in Table III, we give the statistical significance (SS) values by using,

$$SS = \sqrt{2L_{int}\epsilon[(\sigma_S + \sigma_B) \ln(1 + \sigma_S/\sigma_B) - \sigma_S]} \quad (6)$$

where σ_S and σ_B denotes signal and background cross sections in the invariant mass interval of $M_{Z'} - 2\Gamma_{Z'} < M_{tc} < M_{Z'} + 2\Gamma_{Z'}$ by assuming integrated luminosity of $L_{int} = 10^5$ pb $^{-1}$ per year. For the Z' coupling parameter $x = 0.1$, the LHC is able to measure the Z' mass up to about 2 TeV with single top FCNC.

B. The top quark pair production

We investigate the top pair production via Z' boson exchange at the LHC. The Z' boson contributes in the t -channel via the FCNC and in the s -channel through family diagonal neutral current couplings with a strength scaled by the parameter x . The total cross sections

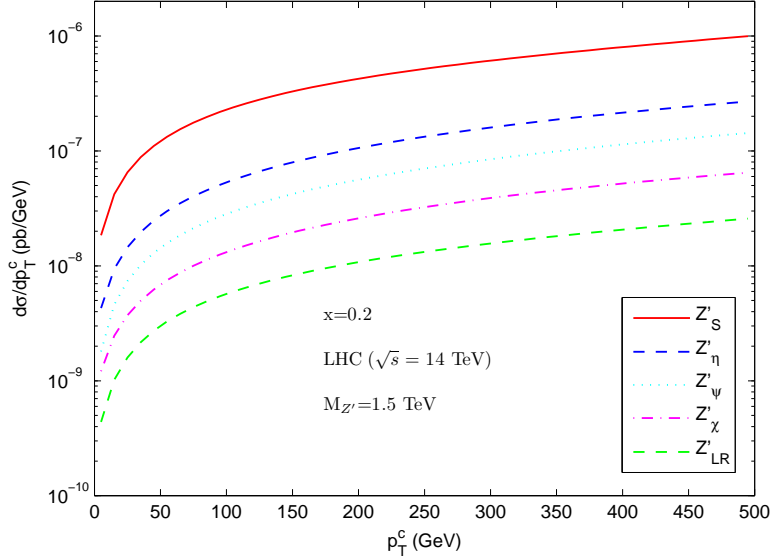


Figure 5: The p_T distribution of the charm quark for the signal process $pp \rightarrow t\bar{c} + \bar{t}cX$ at the LHC ($\sqrt{s} = 14$ TeV) with the FCNC parameter $x=0.2$.

Table III: The signal significance (SS) for the Z' boson predicted in different models, the SS values correspond to the case $x = 0.1$. The integrated luminosity is taken to be $L_{int} = 10^5 \text{pb}^{-1}$.

$M_{Z'}$ (GeV)	Z'_S	Z'_{LR}	Z'_χ	Z'_η	Z'_ψ
700	13.4	18.4	20.3	20.4	20.3
1000	8.0	10.5	11.3	11.6	11.6
1500	4.1	5.2	5.4	5.4	5.4
2000	2.4	2.9	3.0	2.9	2.9
3000	1.4	1.7	1.8	1.8	1.8

for the top pair production with $x = 0.1$ and $x = 1$ for different models of Z' at the LHC are plotted in Fig.8. The main background has the same final state as the signal ($t\bar{t}$). In the invariant mass analysis, we reconstruct the mass of top pairs around the Z' boson mass which are shown in Fig. 9. We assume $t(\bar{t}) \rightarrow W^+(W^-)b(\bar{b})$, where the W bosons decays leptonically. For each of the b -quarks, we assume the b -tagging efficiency as 60%. We calculate the cross section of the background in the mass bin widths for each $M_{Z'}$ value; as an example, for the $M_{Z'} = 1$ TeV we take $\Delta M \simeq 55$ GeV, and we find the background cross section $\Delta\sigma_B = 2.65 \times 10^{-1}$ pb for $pp \rightarrow W^+W^-b\bar{b}X$, and $\Delta\sigma_B = 3.97$ pb for $pp \rightarrow t\bar{t}X$.

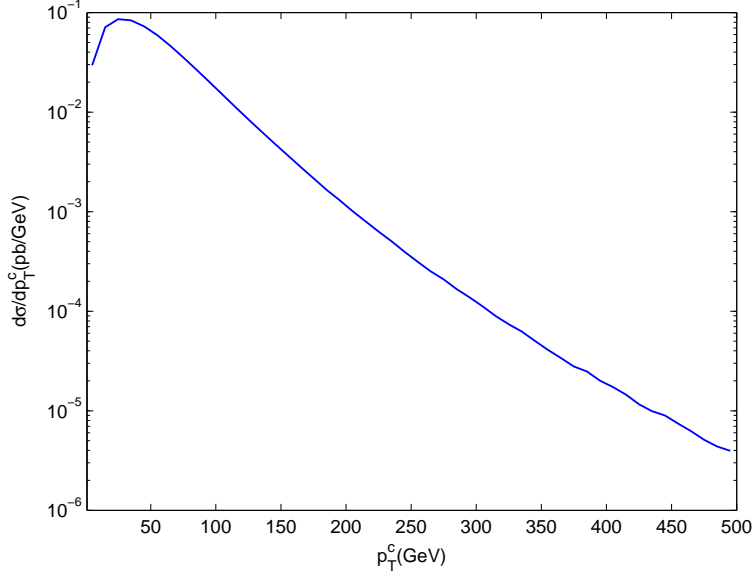


Figure 6: The p_T distribution of the charm quarks (c and \bar{c}) for the background process ($pp \rightarrow t\bar{c} + \bar{t}cX$) at the LHC with $\sqrt{s} = 14$ TeV).

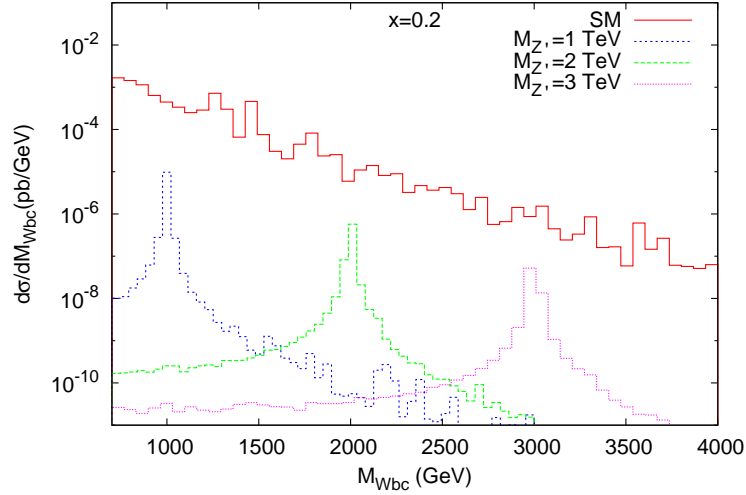


Figure 7: The invariant mass distribution of the $W^+ b \bar{c}$ system for the SM and Z' sequential model with different mass values of Z' at the LHC with $\sqrt{s} = 14$ TeV.

In Table IV, we give the SS values for Z' boson in different models in the case of $x = 0.1(1)$, considering the leptonic channels of the top decays, taking $L_{int} = 100 \text{ fb}^{-1}$.

We plot the 3σ contours in $(x - M_{Z'})$ plane, for different Z' models as shown in Fig. 10 at the LHC with $\sqrt{s} = 14$ TeV and $L_{int} = 150 \text{ fb}^{-1}$. In order to cover all the interested Z'

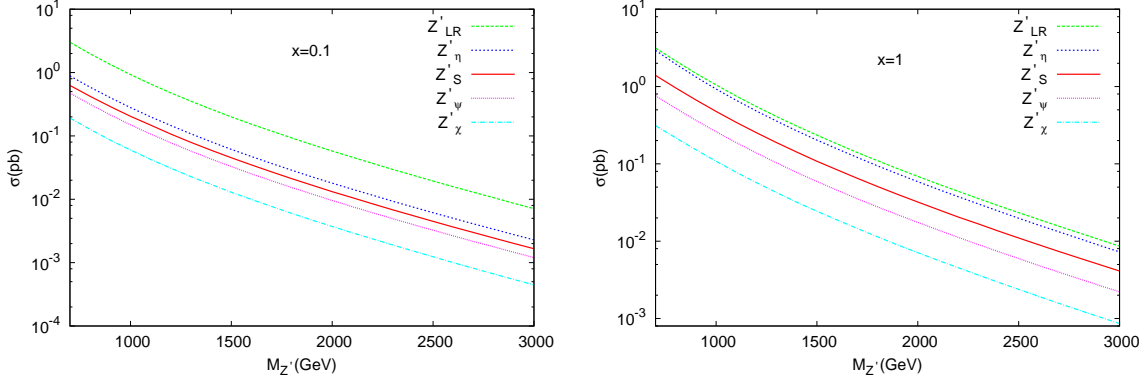


Figure 8: The total cross sections for the top pair production at the LHC (with $\sqrt{s} = 14$ TeV) depending on the Z' mass in the framework of different models with $x = 0.1$ and $x = 1$.

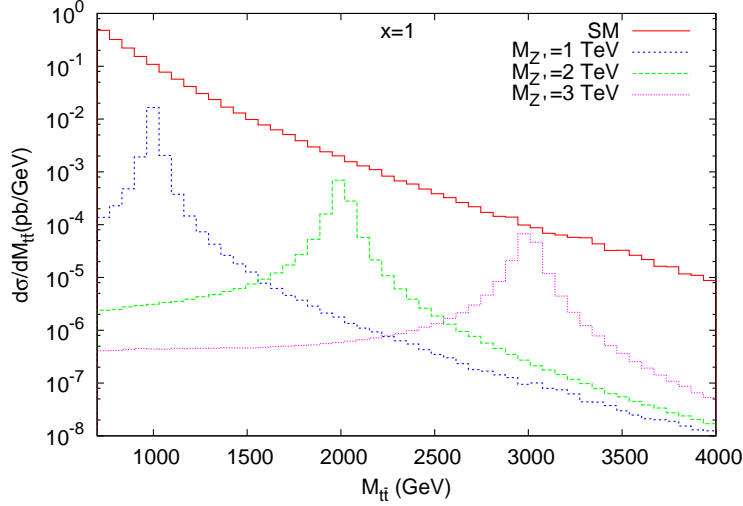


Figure 9: The invariant mass distribution of the top pairs for the SM and sequential Z' model with $x = 1$ at the LHC ($\sqrt{s} = 14$ TeV).

Table IV: The signal significance (SS) for the Z' boson predicted in different models, the SS values show the case $x = 0.1$ (1), with $L_{int} = 100 \text{ fb}^{-1}$.

Mass (GeV)	Z'_S	Z'_{LR}	Z'_χ	Z'_η	Z'_ψ
700	5.6(27.3)	27.0(25.5)	1.7(2.7)	7.9(12.1)	4.3(6.6)
1000	3.6(17.6)	16.2(15.6)	1.0(1.8)	4.9(8.0)	2.6(4.4)
2000	1.2(6.0)	5.3(5.2)	0.3(0.6)	1.6(2.8)	0.9(1.5)
3000	0.5(2.6)	2.3(2.2)	0.1(0.3)	0.7(1.3)	0.4(0.7)

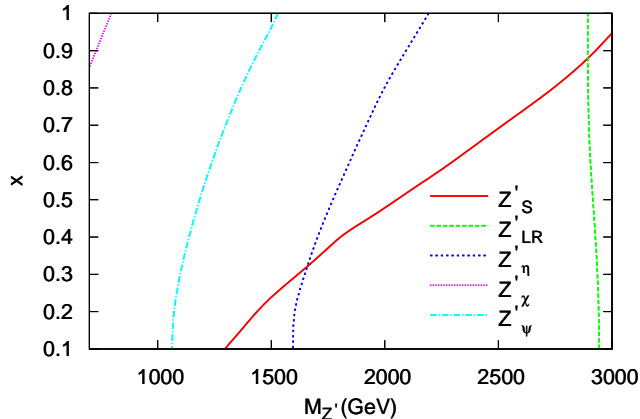


Figure 10: The contour plot for the discovery of Z' boson at the LHC ($\sqrt{s} = 14$ TeV) with $L_{int} = 150$ fb $^{-1}$.

models in the same range of parameter space, we take the integrated luminosity of $L_{int} = 150$ fb $^{-1}$ in the leptonic W -decay channel.

IV. ELECTRON-POSITRON COLLISIONS

We anticipate that the LHC will explore the new physics directions in the ongoing experiments, then the parameters of the new physics will have been known with only moderate precision. The linear collider at a high energy is expected to identify the model parameters and make measurements with great precision beyond the hadron collider reach.

In a lepton collider, the initial state is well known for both unpolarized and polarized beams. The energy-momentum conservation can be used in the full event reconstruction and the energy scan allow precise measurement of the resonance parameters. For the e^+e^- collider, we consider the Compact Linear Collider (CLIC) in two beam acceleration technology allowing the preferable center of mass energy 1(3) TeV with $L = 2(8) \times 10^{34}$ cm $^{-2}$ s $^{-1}$ [5].

A. The single top quark production

The production cross sections for $e^+e^- \rightarrow t\bar{c} + \bar{t}c$ are shown in Fig. 11 at the collision center of mass energy ranging 0.5 – 1.5 TeV with the assumption $M_{Z'} = 1$ TeV. We also

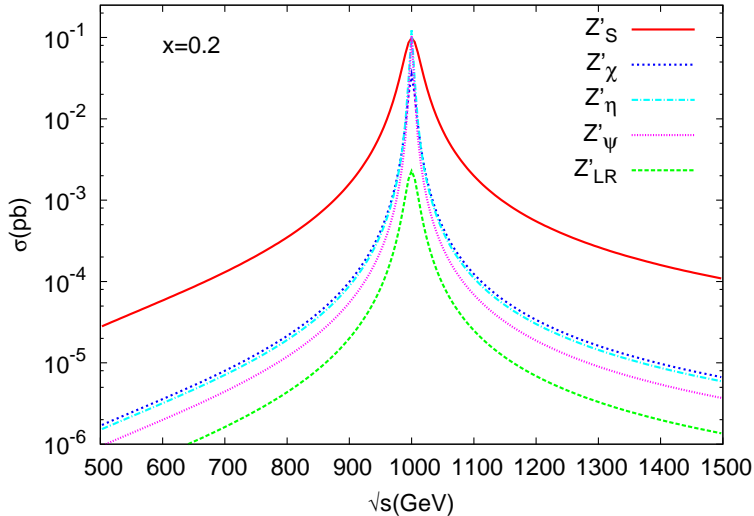


Figure 11: The production cross sections for $e^+e^- \rightarrow t\bar{c} + \bar{t}c$ at the collision center of mass energy range 500-1500 GeV. Here, we set the flavor changing parameter $x = 0.2$. The curves show five models of the Z' boson with mass $M_{Z'} = 1000$ GeV: sequential type (S), left-right symmetrical model (LR), E_6 -inspired models (χ, ψ, η) mentioned in the text.

check our results for $x = 0.1$ with the similar results given in [4]. In Fig. 12, the cross sections around resonance ($M_{Z'} = 3$ TeV) are shown for the center of mass energy range of 2-4 TeV. The sequential model gives the largest cross sections, while the Z'_{LR} model gives the lowest cross section around the resonance in the e^+e^- collisions.

A specific feature of the linear colliders is the presence of initial state radiation (ISR) and beamstrahlung (BS). The effects of the ISR and BS can lead to a decrease in the cross section. Being at the resonance for $M_{Z'} = 3$ TeV, we have the cross sections 9.04×10^{-1} fb (1.93×10^{-2} fb) for sequential (LR) Z' model with $x = 0.2$. Taking center of mass energy $\sqrt{s} = 3$ TeV, and the mass range $1 \text{ TeV} < M_{Z'} < 2.5 \text{ TeV}$ the signal cross sections with the ISR+BS effects are shown in Fig. 13. When calculating the ISR and BS effects, we take updated beam parameters for the CLIC at $\sqrt{s} = 3$ TeV as follows: the beam sizes $\sigma_x + \sigma_y = 46$ nm, bunch length $\sigma_z = 44 \mu\text{m}$, number of the particles in the bunch $N = 3.72 \times 10^9$ [25].

We plot the invariant mass distributions for the $W^+b\bar{c}$ system in the final state, the signal has the peak around $M_{Z'} = 1$ TeV over the smooth background as shown Fig. 14. For each model we can calculate the signal significance using signal and background events in the chosen invariant mass intervals and different mixing parameters x as presented in Table V.

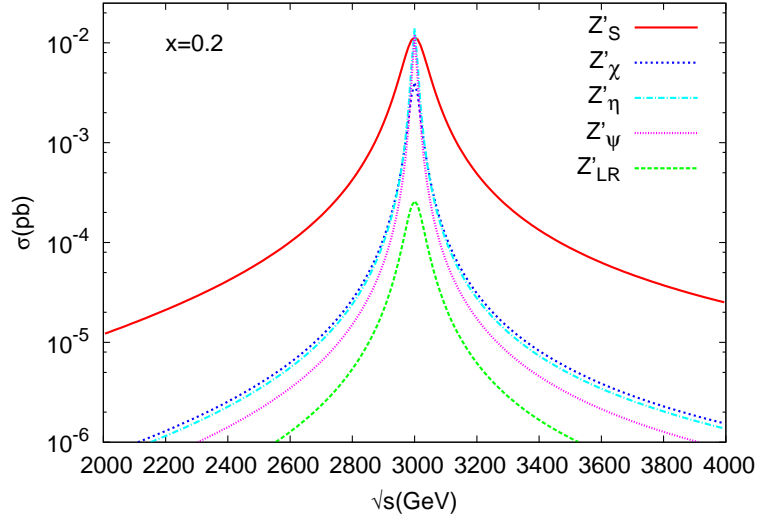


Figure 12: The production cross sections for $e^+e^- \rightarrow t\bar{c} + \bar{t}c$ at the collision center of mass energy range 2000-4000 GeV. Here, we set the Z' boson mass $M_{Z'} = 3000$ GeV and the flavor changing parameter $x = 0.2$. The curves show five models of the Z' boson: sequential type (S), left-right symmetrical model (LR), E_6 -inspired models (χ, ψ, η) mentioned in the text.

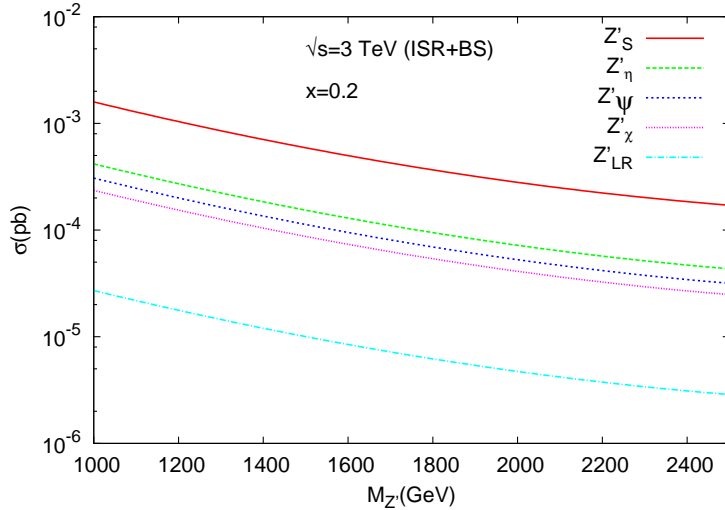


Figure 13: The cross section for the process $e^+e^- \rightarrow t\bar{c} + \bar{t}c$ depending on the Z' mass at $\sqrt{s} = 3$ TeV with the ISR and BS effects.

We require the events lying in the invariant mass intervals $150 \text{ GeV} < M_{Wb} < 200 \text{ GeV}$ and $M_{Z'} - 2\Gamma_{Z'} < M_{Wbc} < M_{Z'} + 2\Gamma_{Z'}$. Assuming Poisson statistics we require $SS > 3$ for signal observation, for this case we can cover almost five Z' models as shown in Fig.

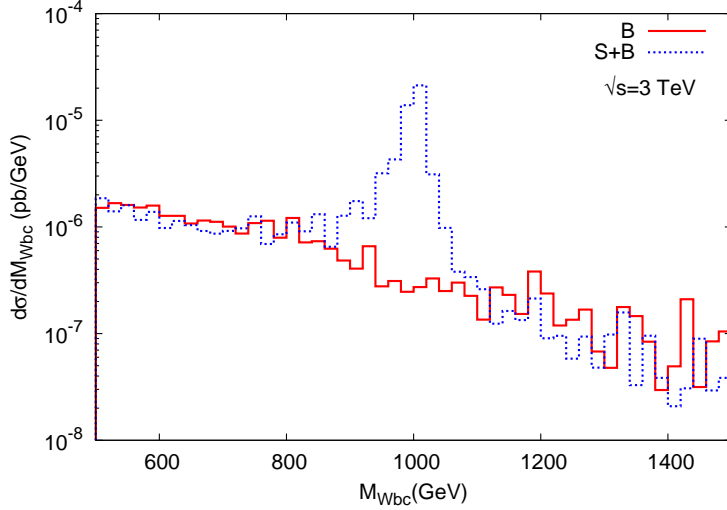


Figure 14: The invariant mass distribution of the $W^+b\bar{c}$ system for the sequential model with $M_{Z'} = 1\text{TeV}$.

Table V: The statistical significance for the Z' search in the single top production at the CLIC ($\sqrt{s} = 3\text{ TeV}$) with $L_{int} = 10^5\text{ pb}^{-1}$. The values are given for $x = 0.1(0.6)$.

Mass (GeV)	Z'_S	Z'_{LR}	Z'_χ	Z'_η	Z'_ψ
700	11.31(4.5)	1.1(0.4)	4.1(1.6)	5.8(2.4)	4.9(2.0)
1000	9.2(2.3)	0.9(0.3)	3.3(1.3)	4.7(1.9)	4.0(1.6)
2000	3.9(1.6)	0.4(0.2)	1.4(0.6)	2.0(0.8)	1.7(0.7)
3000	6.9(2.8)	0.8(0.3)	3.6(1.5)	6.7(2.7)	6.1(2.5)

15. Nevertheless, we need to gather more luminosity (at least a factor of 10) to see more realization of the LR model.

B. The top quark pair production

The Z' boson will enhance the cross section of the pair production of top quarks at the CLIC energies. Having the center of mass energy $\sqrt{s} = 3\text{ TeV}$, we plot the invariant mass distribution of the background and signal (for $M_{Z'} = 1.5, 2$ and 2.5 TeV) as shown in Fig. 16. Here, we consider the process $e^+e^- \rightarrow t\bar{t}$ for both the background and signal. In the analysis, we take into account leptonic decays of the top quarks with the corresponding branchings

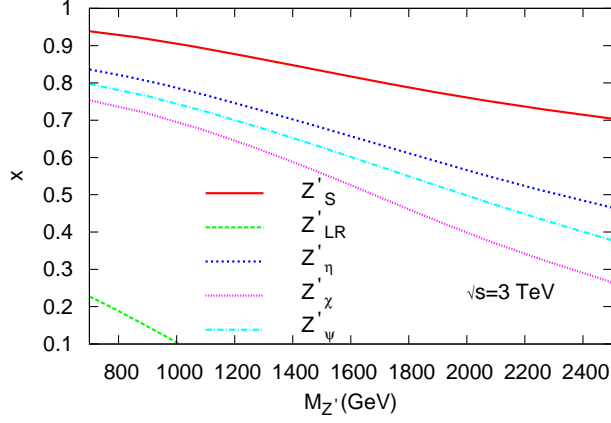


Figure 15: The discovery region for the mass of the Z' boson and the FCNC mixing parameter for the single production of the top quarks.

Table VI: The statistical significance for the Z' search in top pair production at CLIC ($\sqrt{s} = 3\text{TeV}$).

The values are given for $x = 0.1(1)$.

Mass (GeV)	Z'_S	Z'_{LR}	Z'_χ	Z'_η	Z'_ψ
700	71.2(217.6)	161.2(157.3)	69.2(96.6)	112.0(153.3)	92.4(126.7)
1000	53.8(181.7)	126.7(126.8)	155.3(82.3)	87.2(126.8)	73.7(107.7)
2000	26.0(81.9)	55.2(56.0)	24.4(37.7)	37.6(56.7)	32.4(49.1)
3000	50.1(151.4)	115.6(117.3)	67.0(101.0)	137.3(204.6)	122.2(183.4)

and efficiency factors. We also consider the background process $e^+e^- \rightarrow W^+W^-b\bar{b}$, here one can apply the Wb invariant mass cut (around top mass) to reduce this background. We calculate the signal and background events in the invariant mass intervals Δm for an estimation of the signal significance. Taking integrated luminosity $L_{int} = 10^5 \text{ pb}^{-1}$ we calculate statistical significance for the different Z' mass points as shown in Table VI. The discovery region for Z' searches is given in Fig. 17.

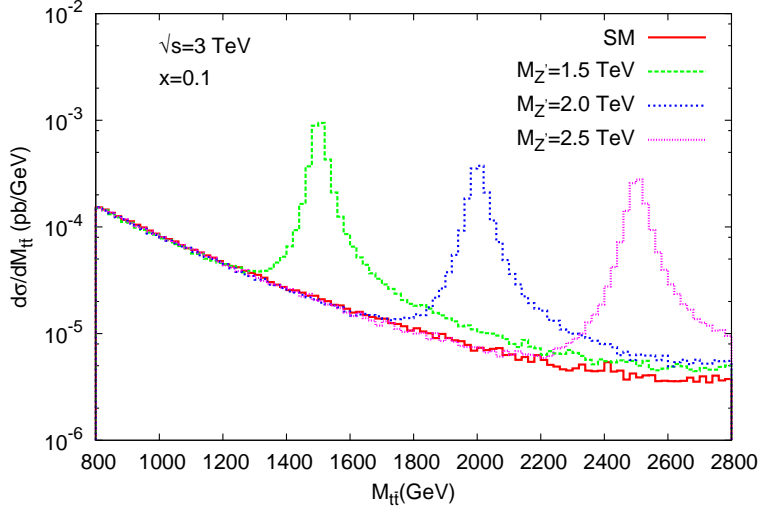


Figure 16: The invariant mass distribution for top pairs in the sequential Z' model at the CLIC with $\sqrt{s} = 3$ TeV.

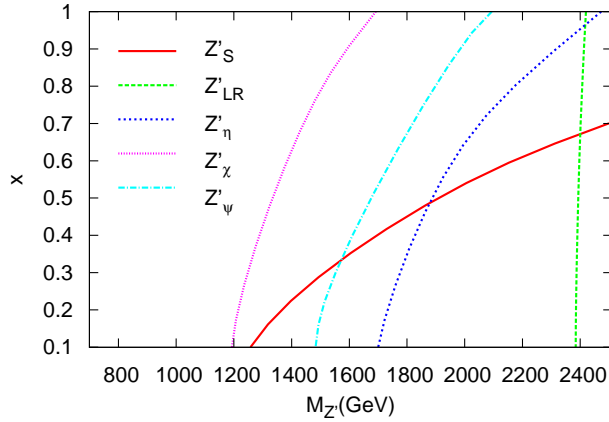


Figure 17: The attainable region for the different Z' models in the $x - m_{Z'}$ plane at the CLIC with $\sqrt{s} = 3$ TeV and $L_{int} = 400$ pb $^{-1}$.

V. ANALYSIS

Heavy quark flavor tagging is useful to analyze the final state event topology. One can identify a heavy flavor jet and measure the invariant mass of the hadrons at a secondary vertex to differentiate the charm and bottom jets. The charm quark hadronizes immediately after it is produced. A charmed jet has a secondary vertex mass ranging from 0 to 2 GeV

with a peak around 1 GeV, while bottom jet has the largest secondary vertex mass with a tail up to 4 GeV. The light quark jets have the smallest secondary vertex masses. In addition, the Monte Carlo samples can be used to determine the fractions of charm, bottom and other light quarks in the event. Here, we assume that one can have success for tagging the charmed meson together with a single top quark. The FCNC single production of top quarks through Z' exchange can be probed at CLIC. For the pair production of top quarks through the Z' contribution, we assumed the b -tagging efficiency as 60% and we use leptonic decay mode of the W -boson.

VI. CONCLUSION

We find the discovery regions of the parameter space for the single and pair FCNC productions of top quarks via Z' exchanges. The tree-level FCNC couplings of the top quark can emerge in the models with an extra $U(1)$ group. In the models considered in this paper, the single and pair production of top quarks at the LHC can have the contributions from the couplings of $Z'q\bar{q}$ and the FCNC couplings of $Z'q\bar{q}'$ (where $q, q' = u, c, t$). For a mixing parameter $x = 0.2$ the LHC can discover top FCNC up to the mass $m_{Z'} = 1.7 - 3$ TeV depending on the Z' models. While at the CLIC, only the $Z't\bar{t}$ interaction contributes to the process $e^+e^- \rightarrow t\bar{t}$ depending on the strength of parameter x . We can also investigate the $Z't\bar{c}$ coupling at the linear colliders independent of the other $Z'q\bar{q}'$ couplings. In case of the resonance production CLIC has better potential than the LHC in searching the single top FCNC via the Z' boson.

Acknowledgments

O.C's work is partially supported by Turkish Atomic Energy Authority (TAEK) under the grant No. CERN-A5.H2.P1.01-10. O.C's work is also partially supported by State Planning Organization (DPT) under the grant No. DPT2006K-120470. I.T.C. acknowledges the support from CERN Physics Department.

[1] P. Langacker, Rev. Mod. Phys. **81**, 1199 (2009).

- [2] C. Amsler *et al.*, Particle Data Group, Phys. Lett. B **667**, 1 (2008).
- [3] J. Erler *et al.*, JHEP 0908, 017 (2009).
- [4] A. Arhrib *et al.*, Phys. Rev. D **73**, 075015 (2006).
- [5] R.W. Assmann *et al.* [The CLIC Study Team], Ed. by G. Guignard, CERN 2000-008; CERN-2003-007; E. Accomando *et al.* [CLIC Physics Working Group], Ed. by M.Battaglia, A.De Roeck, J.Ellis, D.Schulte, CERN-2004-005.
- [6] P. Langacker, M. Plumacher, Phys. Rev. D **62**, 013006 (2000).
- [7] K. Cheung *et al.*, Phys. Lett. B **652**, 285 (2007).
- [8] K. Leroux and D. London, Phys. Lett. B **526**, 97 (2002).
- [9] V. Barger *et al.*, Phys. Lett. B **580**, 186 (2004).
- [10] V. Barger, C. W. Chiang, J. Jiang and P. Langacker, Phys. Lett. B **596**, 229 (2004).
- [11] V. Barger, C. W. Chiang, P. Langacker and H. S. Lee, Phys. Lett. B **598**, 218 (2004).
- [12] C. H. Chen and H. Hatanaka, Phys. Rev. D **73**, 075003 (2006).
- [13] X. G. He and G. Valencia, Phys. Rev. D **74**, 013011 (2006).
- [14] C. W. Chiang, N. G. Deshpande and J. Jiang, JHEP **0608**, 075 (2006).
- [15] S. Baek, J. H. Jeon and C. S. Kim, Phys. Lett. B **641** (2006) 183.
- [16] V. Barger, L. L. Everett, J. Jiang, P. Langacker, T. Liu and C. E. M. Wagner, JHEP **0912**, 048 (2009).
- [17] V. Barger, L. Everett, J. Jiang, P. Langacker, T. Liu and C. Wagner, Phys. Rev. D **80**, 055008 (2009).
- [18] A. Cordero-Cid, G. Tavares-Velasco and J. J. Toscano, Phys. Rev. D **72**, 057701 (2005).
- [19] C. x. Yue, H. j. Zong and L. j. Liu, Mod. Phys. Lett. A **18**, 2187 (2003).
- [20] K. Y. Lee, S. C. Park, H. S. Song and C. Yu, Phys. Rev. D **63**, 094010 (2001).
- [21] C. X. Yue and L. N. Wang, J. Phys. G **34**, 139 (2007).
- [22] F. del Aguila, J. A. Aguilar-Saavedra, M. Moretti, F. Piccinini, R. Pittau and M. Treccani, Phys. Lett. B **685**, 302 (2010).
- [23] A. Pukhov *et al.*, arXiv:hep-ph/9908288.
- [24] J. Pumplin, D. R. Stump, J. Huston, H. L. Lai, P. M. Nadolsky and W. K. Tung, JHEP **0207**, 012 (2002) [arXiv:hep-ph/0201195].
- [25] H. Braun *et al.*, CLIC Study Team, CERN-OPEN-2008-021, CLIC-Note-764 (2008).